Archives of Biochemistry and Biophysics
Vol. 371, No. 1, November 1, pp. 1–7, 1999
Article ID abbi.1999.1412, available online at http://www.idealibrary.com on IDEAL®

AFM Study of Membrane Proteins, Cytochrome P450 2B4, and NADPH–Cytochrome P450 Reductase and Their Complex Formation

Olga I. Kiselyova,* Igor V. Yaminsky,* Yuri D. Ivanov,†,[1] Irina P. Kanaeva,† Vadim Yu. Kuznetsov,† and Alexander I. Archakov†

**Faculty of Physics, Moscow State University, Moscow, Russia; and*
†Institute of Biomedical Chemistry RAMS, Moscow, Russia

Received March 8, 1999, and in revised form July 26, 1999

The application of the AFM technique for visualization of membrane proteins and for measuring their dimensions was demonstrated. The AFM images of the microsomal monooxygenase system components—cytochrome P450 2B4 and NADPH–cytochrome P450 reductase—were obtained by using two types of supports—hydrophobic, highly oriented pyrolytic graphite (HOPG) and hydrophilic mica. It was shown that hemo- and flavoprotein monomers and oligomers can be adsorbed to and visualized on HOPG. On the negatively charged mica matrix, flavoprotein oligomers dissociated to monomers while hemoprotein oligomers dissociated into less aggregated particles. The images of cytochrome P450 2B4 and NADPH–cytochrome P450 reductase monomers were about 3 and 5 nm high, respectively, while the images of oligomeric forms of these proteins were about 10 and 8 nm high, respectively. We were able to observe the binary complexes composed of monomeric proteins, cytochrome P450 2B4 and its reductase and to measure the heights of these complexes (7 nm). The method is applicable for visualization of not only individual proteins but also their complexes.

Key Words: **cytochrome P450 2B4; NADPH–cytochrome P450 reductase; oligomers; monomers; atomic force microscopy (AFM); complex formation.**

The cytochrome P450-containing microsomal monooxygenase system plays the key role in the metabolism of drugs, carcinogens, mutagens, and other xenobiotics (1). As known, cytochrome P450 2B4 (2B4)[2] functions by interacting with its redox partner, NADPH–cytochrome P450 reductase (Fp). Both 2B4 and Fp are membrane proteins which hampers the study of their functions. When solubilized from the microsomal membrane, Fp and 2B4 become oligomeric (2–4). To make them monomeric, a detergent monomerization technique was developed (5). Various experimental methods are currently used for determination of protein sizes and weights such as sedimentation, gel chromatography, electrophoresis, correlation laser scattering, and others (2, 3, 5). Recently, the atomic force microscopy (AFM) and scanning tunneling techniques (STM) have been put to use for size measuring and visualization of individual nanomeric objects—such as nucleic acids, biological membranes, protein crystals (6), photosynthetic reaction centrum (7), clathrin (8), concanavalin A (9), and NADPH–cytochrome P450 reductase (10). In the present work, the AFM study of oligo- and monomeric 2B4 and FP, as well as 2B4/Fp complexes, was performed by using hydrophobic (graphite) and hydrophilic (mica) supports. The 2B4 and Fp monomers and oligomers can be visualized on graphite support. It was shown that electrostatic protein–support interactions play an essential role in the dissociation of 2B4 and Fp oligomers on mica. The binary complexes formed from 2B4 and Fp monomers were only observed on the mica support.

MATERIALS AND METHODS

Chemicals. Emulgen 913 was purchased from Kao Atlas (Osaka, Japan). Other chemicals were purchased from Reakhim (Moscow, Russia).

[1] To whom correspondence should be addressed at Institute of Biomedical Chemistry RAMS, Pogodinskaya St. 10, Moscow, 119832, Russia.

[2] Abbreviations used: 2B4, cytochrome P450 2B4; Fp, NADPH–cytochrome P450 reductase; HOPG, highly oriented pyrolytic graphite; AFM, atomic force microscopy.

0003-9861/99 $30.00

Preparation of proteins. Oligomers of membrane proteins 2B4 and Fp were isolated from liver microsomes of male New Zealand rabbits treated with 0.1% (w/v) sodium phenobarbital in drinking water for 1 week as described earlier (11, 12). Specific content and specific activity of Fp at 30°C were 13–13.5 nmol Fp ★ mg^{-1} protein and 40–43 μmol of cytochrome c ★ min^{-1} ★ mg^{-1} protein, respectively. Specific content of 2B4 was 17–18 nmol ★ mg^{-1} protein and its $A_{276}/A_{418} = 1$. Both proteins showed a single band on SDS–PAGE.

Monomerization of Fp and 2B4 oligomers was carried out as follows: to 5 nmol (20–30 μl) of either protein 13 μl of 2% (w/v) Emulgen 913 solution was added. After 10 min incubation at room temperature, the protein and Emulgen 913 concentrations were brought to 5 μM and 0.25 g/liter, respectively, with 100 mM K-phosphate (KP) buffer, pH 7.4, and the mixtures were incubated at 4°C for another 24 h (5).

Analytical measurements. The concentration of 2B4 was determined by the method of Omura and Sato (13) using the extinction coefficient of $A_{450-490} = 91\ mM^{-1}\ cm^{-1}$ for the CO complex of the oxidized minus reduced 2B4 in the difference spectrum. The concentration of purified Fp was determined using the extinction coefficient of $A_{456} = 21.4\ mM^{-1}\ cm^{-1}$ (14).

AFM experiments and samples preparation. Experiments were carried out using the direct surface adsorption method (15). As supports, HOPG and mica were used. The solution of 2B4 or Fp monomers (5 μM) in 100 mM KP buffer with 0.25 g/liter Emulgen 913 was diluted with the same buffer up to 0.2 μM. Protein samples were deposited on the HOPG or mica surface and left for 2 min. Then each sample was rinsed with distilled water and dried in air flow. The 2B4/Fp complexes were obtained by mixing appropriate monomeric proteins in solution at the concentration for each protein of 5 μM in 100 mM KP buffer, pH 7.4, with 0.25 g/liter Emulgen. Then the mixture was incubated for 10 min, diluted 50 times in the same buffer, and immediately placed onto support. According to the data reported earlier (16), with the air humidity 45% and higher, the mica surface is covered with water layer. In this study, samples were imaged in air under ambient conditions, with relative humidity being 60–70%. There is reason enough to suppose that the protein molecules under study remain hydrated.

All AFM experiments were carried out in the tapping mode on a multimode Nanoscope IIIa atomic force microscope (Digital Instruments, Santa Barbara, CA). Commercially available Nanoprobe cantilevers for the tapping mode (Digital Instruments) were used. The length of the cantilevers was 125 μm and the resonant frequency was 308–340 kHz.

AFM images were processed with the aid of the user-friendly software Femtoscan 001 (Advanced Technologies Center, Moscow, Russia) (17).

RESULTS AND DISCUSSION

AFM is a novel high-resolution instrument for nanometer-scale objects size measuring and visualization (6). An important property of AFM is its ability to measure the exact height of observed rigid objects. The lateral dimensions are broadened due to a tip-related effect (18). Therefore, the main criterion for distinguishing between the monomeric and oligomeric protein forms is the height of the observed object. The images of objects have bell-shape profiles. The diameter of an object was determined as the width of its bell-shaped image measured at half height. For control experiments the appropriate buffer mixture without proteins was applied to a support and imaged. Randomly distributed contaminations in control measurements were less than 1 nm high.

Visualization of oligomeric and monomeric 2B4 and Fp images and of their complexes was carried out on two types of surfaces—hydrophobic HOPG and hydrophilic mica. The choice of protein concentration was dictated by the demands of the AFM technique: high concentrations (about 5 μM) lead to the adhesion of too many molecules to the surface; they cover the surface by multilayers which do not ensure good resolution. In view of this, the protein concentrations used were lower than 5 μM.

As was shown earlier, the incubation of Fp or 2B4 oligomers in 100 mM KP buffer, pH 7.4, with 0.25 g/liter Emulgen 913 led to their dissociation to monomers (5). The images of 2B4 monomers on HOPG are presented in Figs. 1A and 1B. Here and further in the AFM images darker regions correspond to pits and lighter regions correspond to protrusions. The measured dimensions of these protrusions were approximately 2.5–3 nm high and 15–18 nm in diameter. As the maximum height of imaged contaminations in KP buffer does not exceed 1 nm, the protrusions of 2.5–3 nm in height may be considered as proteins. The conclusion about the monomeric state of 2B4 (Figs. 1 A and 1B) is based on the assumption that the molecular size of 2B4 is close to that of cytochrome P450cam whose height and width as measured by X-ray analysis are, respectively, 3 and 5 nm (index PDB 2CPP) (19). The enlarged lateral diameter of 2B4 images—15 to 18 nm—is apparently due to the tip-induced broadening effect (18). The monomers are better visualized and are more contrasting in 20 mM KP buffer, pH 7.4, containing 0.25 g/liter Emulgen 913 (Fig. 1B) than in 100 mM KP buffer at the same detergent concentration (Fig. 1A). It appears that monomers adsorption occurs better at low rather than high buffer ionic strength. The three-dimensional image of monomers (light color) in Fig. 1B (bottom) is shown for illustration and better comprehension of the image perspective.

We could not obtain the images of 2B4 monomers on hydrophilic mica support—in view of slight binding of hydrophobic protein molecules to the negatively charged hydrophilic surface.

Figure 1C represents the images of 2B4 oligomers on HOPG. Comparison of Figs. 1A, 1B, and 1C reveals essential differences between the images of oligomers and monomers. In Fig. 1C oligomers show up as globules with unresolved structure (white spots). The measured height of these oligomers is about 10 nm and their average diameter is about 50 nm. By comparing the heights of oligomers and monomers, the volume of oligomers was calculated. It was 48 times larger than that of monomers. It was supposed therefore that each oligomer consists of 40–60 molecules of monomers. Thus, the volume (V_m) occupied by a 2B4 monomer with radius r_m is

$$V_m = (4/3)\pi r_m^3 \qquad [1]$$

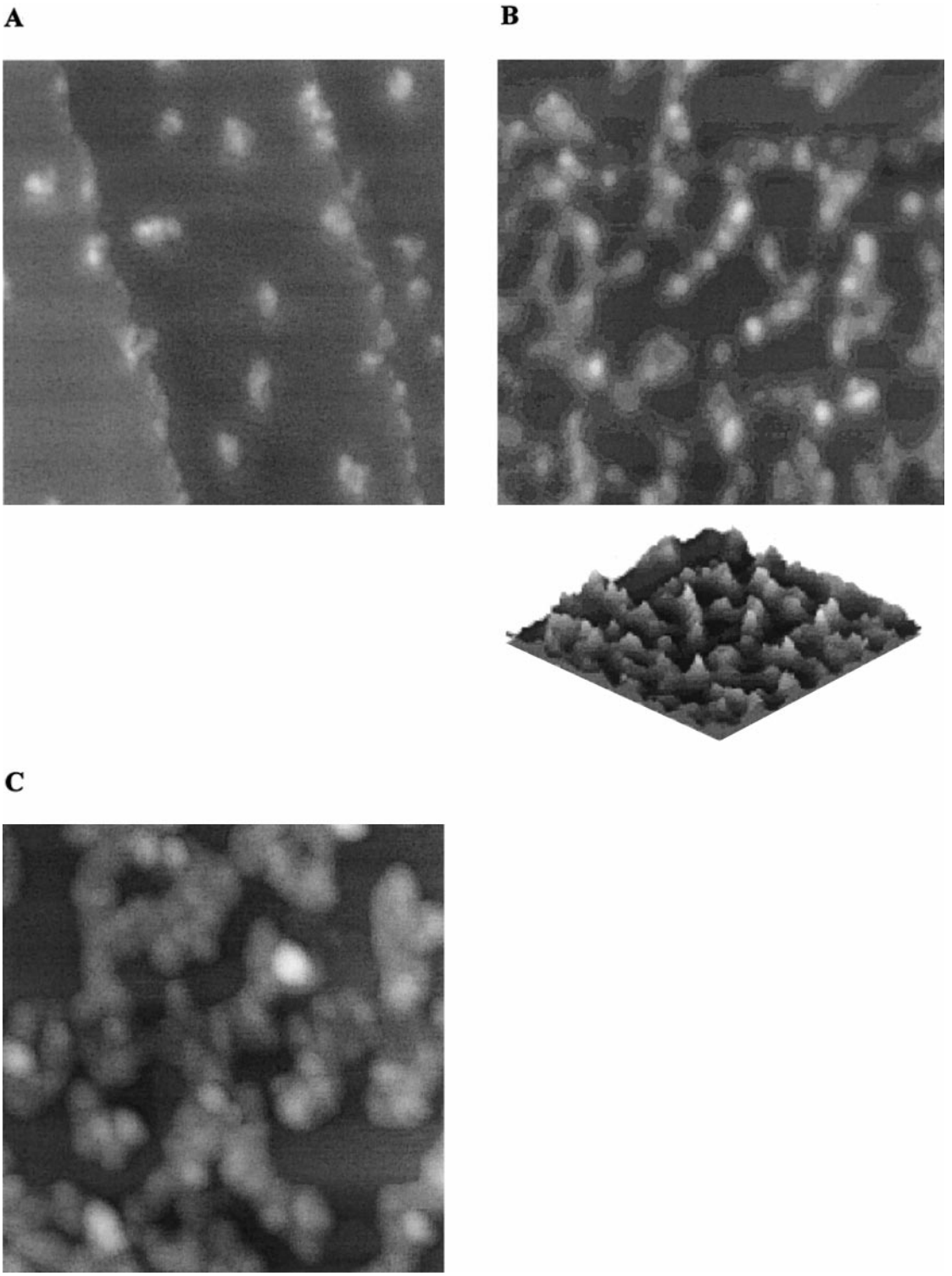

FIG. 1. AFM images of 2B4 monomers (A, B) and oligomers (C) on HOPG. In B, their three-dimensional image is also presented. The experimental conditions were 0.2 μM 2B4 in 100 mM KP buffer, pH 7.4, with 0.25 g/liter Emulgen 913 (A); 0.2 μM 2B4 in 20 mM KP buffer, pH 7.4, with 0.25 g/liter Emulgen 913 (B); and 0.5 μM 2B4 in 100 mM KP buffer, pH 7.4 (C). The image areas were 0.8 $\times$ 0.8 μm (A, B) and 1.0 $\times$ 1.0 μm (C).

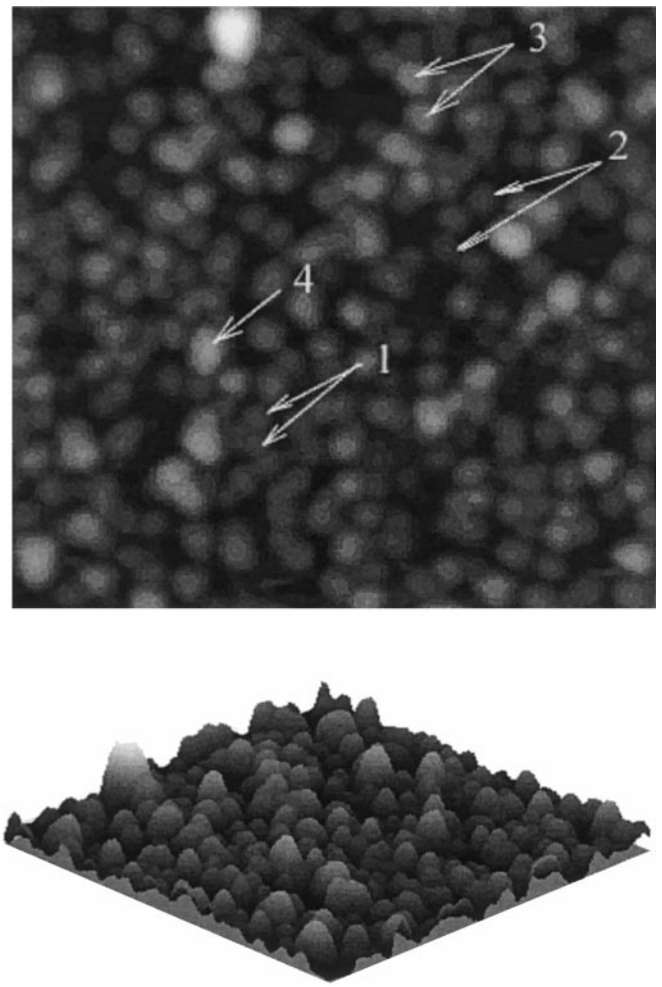

FIG. 2. Two-dimensional (top) and three-dimensional (bottom) AFM images of 2B4 oligomers on mica. The experimental conditions were 1.7 μM 2B4 in 100 KP buffer, pH 7.4. The image area was 0.48×0.48 μm. Arrows 1–4 indicate groups of protrusions presented in Table I.

while the volume occupied by n monomers in the oligomer (in the approximation neglecting the space between its monomeric units) may be expressed as

$$V_o = nV_m. \quad [2]$$

Assuming that the height of the monomer (h_m) or oligomer (h_o) is $2r_{m,o}$, we obtain

$$n = V_o/V_m = (h_o/h_m)^3. \quad [3]$$

Two-dimensional (top) and three-dimensional (bottom) views of 2B4 oligomers on mica in 100 mM KP buffer, pH 7.4, are shown in Fig. 2. Unlike monomers, which cannot be adsorbed on mica support, oligomers demonstrate high adhesion to mica. Apparently, the 2B4 oligomer images on mica differ greatly from those on HOPG. On mica, apart from large 50-nm protrusions, a number of small-sized images are seen. According to the sizes, all protrusions can be divided into four groups as represented in Table I. It seems to us natural to refer to the particles of the first group as monomers, since the height of these 2B4 molecules is approximately 2.5–3 nm and their diameter is 15 nm. The second group of particles was defined as octamers (n = 8 was calculated from Eq. [3] using the average h_m = 2.75 nm and h_o = 5.5 nm). The rest of the particles were considered as those being at a higher oligomerization level. Comparing Figs. 1C and 2, one can see that a hydrophilic, negatively charged mica surface promotes dissociation of 2B4 oligomers to the less aggregated particles. The dissociation of oligomers may be explained by the fact that electrostatic interactions between the charged groups of 2B4 molecules and charged mica support are more intensive than the intermolecular interactions between 2B4 molecules in their oligomeric complexes. On HOPG, the hydrophobic interactions between 2B4 molecules and the hydrophobic surface of the matrix are insufficient for dissociation of the oligomeric complex to occur.

The images of Fp monomers on HOPG are presented in Fig. 3A. The space-separated objects are clearly seen. The imaged Fp molecules are 4–5 nm high and 20–22 nm in diameter. It is known that sizes of Fp without its hydrophobic tail are 5 nm deep $\times$ 7 nm wide $\times$ 6 nm high (20). Indeed, the 4- to 5-nm height of the particles observed agrees well with the expected size for monomeric Fp. The images of Fp monomers were unobtainable on mica because of poor adsorption of hydrophobic molecules on the mica surface. Images of oligomeric Fp on HOPG are represented in Fig. 3B. Oligomers cohere with each other forming a two-dimensional network. Clearly, oligomeric images shown in Fig. 3B differ greatly from monomeric Fp images (Fig. 3A). The average height of Fp oligomer images was about 7–8 nm, and their diameter was 40–60 nm. Based on Eq. [3], where the average h_m = 4.5 nm for Fp monomers and the average h_o = 7.5 nm for Fp oligomers, we suggest that each oligomer consists of five monomers. In contrast to monomers, high affinity of Fp

TABLE I

Sizes and Surface Concentrations of 2B4 Monomers and Oligomers on Mica Surface

N of group	Height (nm)	Average diameter (nm)	Number per square unit	N-merization
1	2.5–3	15–18	100	Monomer
2	5–6	22–25	35	8-mer
3	8–9	22–37	10	12- to 30-mer
4	12–15	50–60	0.5	Aggregates of higher orders

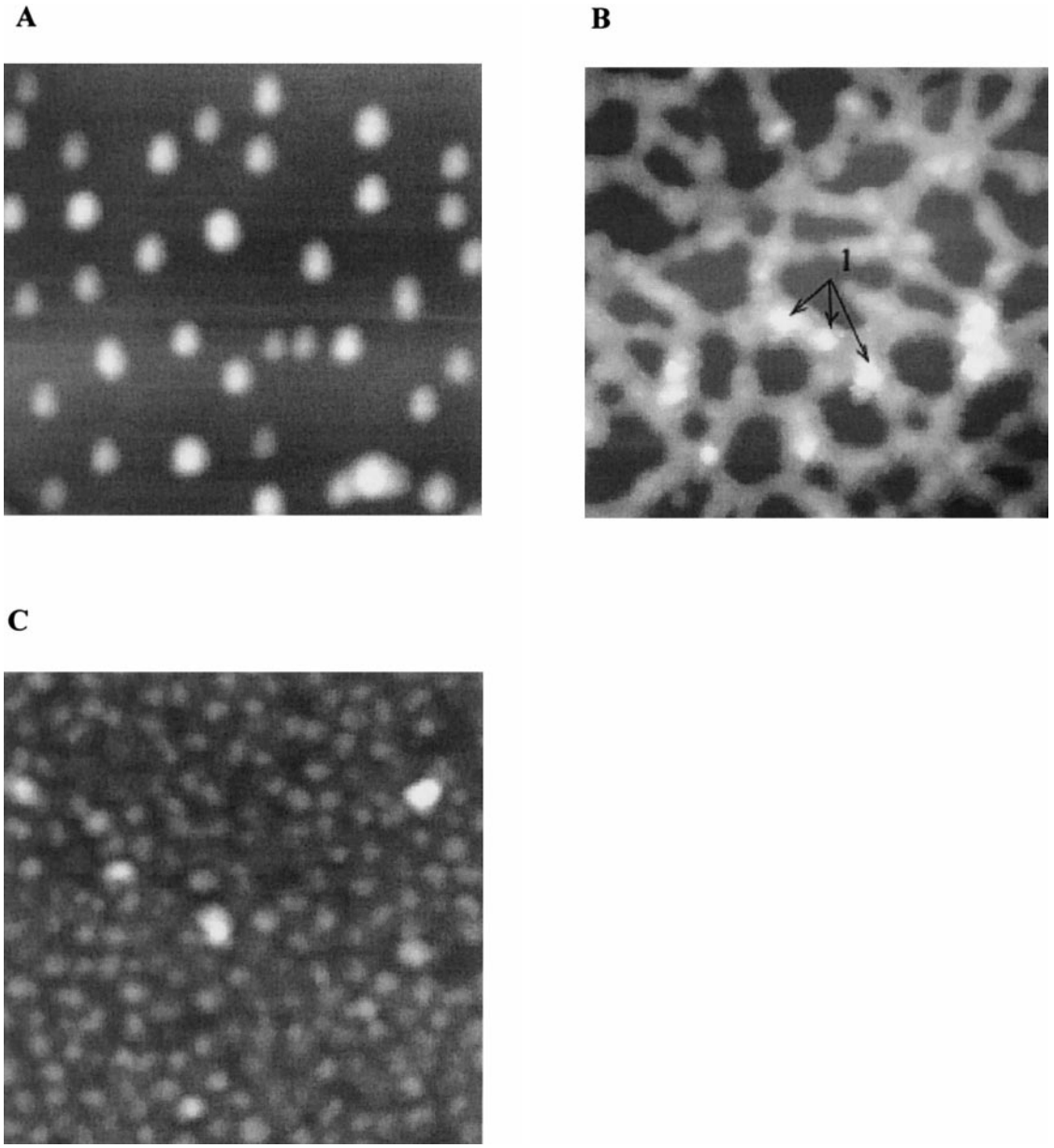

FIG. 3. AFM images of Fp monomers (A) and oligomers (B) on HOPG and Fp oligomers on mica (C). The experimental conditions were 0.2 μM Fp in 100 mM KP buffer, pH 7.4, with 0.25 g/liter Emulgen 913 (A) and 0.2 μM Fp in 100 mM KP buffer, pH 7.4 (B, C). The image areas were 0.8 $\times$ 0.8 μm (A), 1.1 $\times$ 1.1 μm (B), and 0.5 $\times$ 0.5 μm (C).

oligomers to mica support was registered. The interaction between the negatively charged mica support and Fp monomers in oligomer was so strong that only Fp monomers were seen, most of them being 4–5 nm high and 20–22 nm in diameter (Fig. 3C). The dissociation of Fp oligomers on mica suggests that electrostatic Fp–mica interactions surpass the attraction between Fp molecules in oligomers. The dissociation of Fp and 2B4 oligomers to less aggregated particles is probably explained by mica-induced stripping of monomers from the aggregates with their subsequent spreading on the mica surface.

We believe that impossibility for 2B4 and Fp monomers to adsorb on mica is explained by weak adhesion of monomers whose hydrophobic sites are covered with detergent. In the case of aggregates their solutions do not contain Emulgen 913; therefore, the interactions of monomeric subunits comprising the aggregate with the mica surface occur at the expense of electrostatic forces, which allows distinct subunits to adsorb on mica.

At the same time, the Fp/2B4 complexes on mica were readily obtainable (Fig. 4). As seen from Table I, the 2B4 aggregates on mica were divided, according to height, into four groups (with heights 2.5–3, 5–6, 8–9, and 12–15 nm), while Fp aggregates on mica were only visualized as 4- to 5-nm monomers. With 2B4/Fp complexes on mica (Table II), the images with heights 2.5–3, 4–5, 6–8, and 10 nm and higher were distinguished. Comparing the data in Tables I and II, one can see that a new group of objects emerges whose height is about 6–8 nm; the objects of such height were not observable among aggregate images—where only uniform proteins were seen. Taking into account that (a) the height of the complexes is greater than the heights of individual monomers, 2B4 (2.5–3 nm, Fig. 1A)–Fp (4–5 nm, Fig. 3A), and (b) the height of the binary complex is roughly equal to the sum of heights of the monomeric 2B4 and Fp, it was concluded that these elongated objects are, in fact, the binary 2B4/Fp complexes. The presence of 2B4 and Fp monomers in mixed solution (Fig. 4), along with their absence from one-component solutions, is evidence for the dissociation of the 2B4/Fp complex at the cost of strong electrostatic interactions between its constituent monomers and the mica surface.

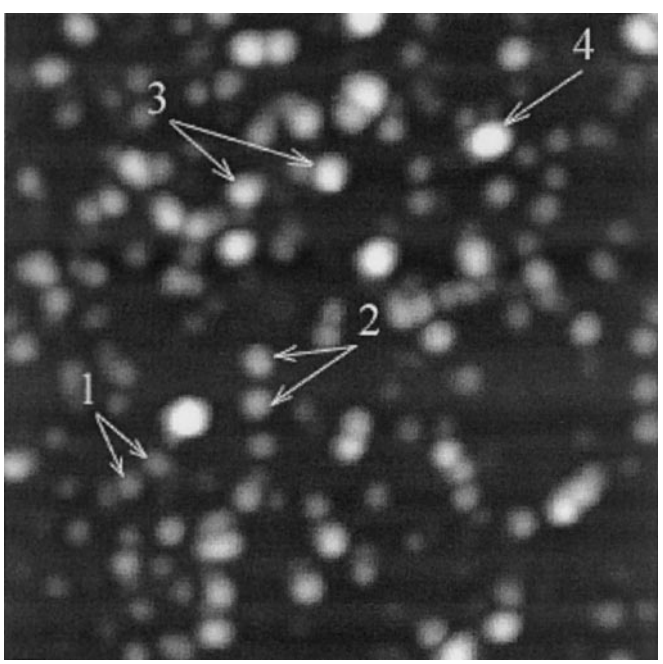

FIG. 4. AFM images of 2B4/Fp complexes on mica. The experimental conditions were 0.2 μM of each protein in 100 mM KP buffer, pH 7.4, with 0.25 g/liter Emulgen 913. The image area was 0.54 × 0.54 μm. Arrows 1–4 indicate the images of 2B4 monomers, Fp monomers, binary complexes of 2B4/Fp monomers, and aggregates of higher orders, respectively.

TABLE II

Sizes and Complex Types for the 2B4/Fp Redox Pair

N of group	Height (nm)	Average diameter (nm)	Type of complex
1	2.5–3	15–18	2B4 monomer
2	4–5	20–22	Fp monomer
3	6–8	25–30	2B4/Fp
4	10 and greater	35 and greater	Aggregates of higher orders

CONCLUSION

In the present study the potential of the AFM technique for visualization of membrane proteins, 2B4 and Fp, and their complexes was demonstrated. The images of 2B4 and Fp monomers and oligomers were obtained on hydrophobic HOPG. With the use of the hydrophilic mica matrix, neither 2B4 nor Fp monomers were visualized; at the same time, the imaging of 2B4 and Fp oligomers revealed their dissociation into less aggregated particles. The binary complexes, comprising 2B4 and Fp monomers, were first visualized on the mica support.

ACKNOWLEDGMENTS

This work was supported by the Russian Foundation for Basic Research (RFBR) Grants N 95-04-12515a and N 96-04-49691.

REFERENCES

1. Archakov, A. I., and Bachmanova, G. I. (1990) Cytochrome P450 and Active Oxygen, Taylor & Francis, London, New York, Philadelphia.
2. Tsuprun, V. L., Myasoedova, K. N., Berndt, P., Sograph, O. I., Chernyak, V. Yu., Archakov, A. I., and Skulachev, V. P. (1985) *Docl. AS USSR* **285,** 1496–1499.
3. Dean, W. L., and Gray, R. D. (1982) *J. Biol. Chem.* **257,** 14679–14685.
4. Wagner, S. L., Dean, W. L., and Gray, R. D. (1984) *J. Biol. Chem.* **259,** 2390–2395.
5. Kanaeva, I. P., Dedinskii, I. R., Skotselyas, E. D., Krainev, A. G., Guleva, I. V., Sevrukova, I. F., Koen, Y. M., Kuznetsova, G. P., Bachmanova, G. I., and Archakov, A. I. (1992) *Arch. Biochem. Biophys.* **298,** 395–402.
6. Hansma, H. G., and Hoh, J. H. (1994) *Annu. Rev. Biomol. Struct.* **23,** 115–139.
7. Alekperov, S. D., Vasil'ev, S. I., Kononenko, A. A., Lukashov, E. P., Panov, V. I., and Semenov, A. E. (1988) *Docl. AS USSR* **303,** 341–344.
8. Wagner, P., Kernen, P., Hegner, M., Ungewickell, E., and Semenza, G. (1994) *FEBS Lett.* **356,** 267–271.
9. Horber, J. K. H., Lang, C. A., Hansch, T. W., Heckl, W. M., and Mohwald, H. (1998) *Chem. Physics Lett.* **145,** 151–158.
10. Bayburt, T. H., Carlson, J. W., and Sligar, S. G. (1998) *J. Struct. Biol.* **123**(1), 37–44.
11. Karuzina, I. I., Bachmanova, G. I., Mengasetdinov, D. E., Myasoedova, K. N., Zhikhareva, V. O., Kuznetsova, G. P., and Archakov, A. I. (1979) *Biokhimia* **44,** 1049–1057.

12. Kanaeva, I. P., Skotselyas, E. D., Kuznetsova, G. P., Antonova, G. N., Bachmanova, G. I., and Archakov, A. I. (1985) *Biokhimia* **50,** 1382–1388.
13. Omura, T., and Sato, R. (1964) *J. Biol. Chem.* **239,** 2370–2385.
14. French, J. S., and Coon, M. G. (1979) *Arch. Biochem. Biophys.* **195,** 565–577.
15. Yang, J., Mou, J., and Shao, Z. (1994) *Biochim. Biophys. Acta* **1199,** 105–114.
16. Guckenberger, R., Heim, M., Cevc, G., Knapp, H. F., Wiegrabe, W., and Hillerbrand, A. (1994) *Science* **266,** 1538–1540.
17. Filonov, A. S., and Yaminsky, I. V. (1997) SPM control and image processing software, Advanced Technologies Center, Moscow.
18. Bustamante, C., Vesenka, J., Tang, C. L., Lees, W., Guthold, M., and Keller, R. (1992) *Biochemistry* **31,** 22–26.
19. Bernstein, F. C., Koetzle, T. F., Williams, G. J. B., Meyer, E. F., Brice, M. D., Rodgers, J. R., Kennard, O., Shimanouchi, T., and Tasumi, M. (1977) *J. Mol. Biol.* **112,** 535–542.
20. Wang, M., Roberts, D. L., Paschke, R., Shea, T. M., Masters, B. S. S., and Kim, J. J. P. (1997) *Proc. Natl. Acad. Sci. USA* **94,** 8411–8416.